

Interactions between myocardial sympathetic denervation and left ventricular mechanical dyssynchrony: A CZT analysis

Alessia Gimelli, MD,^a Riccardo Liga, MD,^b Francesca Menichetti, MD,^c
Ezio Soldati, MD,^c Maria Grazia Bongiorno, MD,^c and Paolo Marzullo, MD^{a,d}

^a Fondazione Toscana Gabriele Monasterio, Pisa, Italy

^b University of Pisa, Pisa, Italy

^c Cardio-Thoracic and Vascular department, University Hospital of Pisa, Pisa, Italy

^d CNR, Institute of Clinical Physiology, Pisa, Italy

Received Jun 1, 2017; accepted Aug 2, 2017

doi:10.1007/s12350-017-1036-3

Background. A correlation between left ventricular (LV) dyssynchrony (LVD) and impaired myocardial sympathetic tone has been hypothesized. We sought to assess the interactions between regional LV sympathetic innervation, perfusion, and mechanical dyssynchrony.

Methods. Eighty-three patients underwent evaluation of LV perfusion and sympathetic innervation on ^{99m}Tc-tetrofosmin/¹²³I-metaiodobenzylguanidine (¹²³I-MIBG) imaging. The summed rest score and summed ¹²³I-MIBG score (SS-MIBG) were computed. The extent of “innervation/perfusion” mismatch was defined as the number of denervated LV segments with relatively preserved perfusion. LVD was evaluated on phase analysis and the wall with latest mechanical activation identified.

Results. LVD was revealed in 36 (43%) patients. Patients with LVD had more abnormal values of SRS (21 ± 9 vs 10 ± 8, *P* < 0.001) and SS-MIBG (29 ± 9 vs 17 ± 11, *P* < 0.001) than those without LVD. The presence of LVD also clustered with a higher burden of “innervation/perfusion” mismatch (*P* = 0.019). On per-wall analysis, LV walls with delayed mechanical activation showed a higher burden of “innervation/perfusion” mismatch (2.3 ± 1.4 segments) than normally contracting walls (1.3 ± 1.2 segments; *P* < 0.001). On multivariate analysis, the extent of “innervation/perfusion” mismatch was the only predictor of delayed mechanical activation (*P* = 0.029).

Conclusions. Patients with LVD show an elevated burden of “innervation/perfusion” mismatch that is concentrated at the level of the most dyssynchronous walls. (*J Nucl Cardiol* 2019;26:509–18.)

Key Words: ¹²³I-metaiodobenzylguanidine • left ventricular dyssynchrony • CZT • innervation/perfusion mismatch • phase analysis

Abbreviations		¹²³ I-MIBG	¹²³ I-metaiodobenzylguanidine
SPECT	Single-photon emission computed tomography	SRS	Summed rest score
CZT	Cadmium-zinc-telluride	SS-MIBG	Summed ¹²³ I-MIBG score
LVD	Left ventricular dyssynchrony	SD	Standard deviation

See related editorial, pp. 519–523

Electronic supplementary material The online version of this article (doi:10.1007/s12350-017-1036-3) contains supplementary material, which is available to authorized users.

The authors of this article have provided a PowerPoint file, available for download at SpringerLink, which summarizes the contents of the paper and is free for re-use at meetings and presentations. Search for the article DOI on SpringerLink.com.

Drs Gimelli and Liga have contributed equally to the study and share the first co-authorship.

Reprint requests: Alessia Gimelli, MD, Fondazione Toscana Gabriele Monasterio, Via Moruzzi, 1, 56124 Pisa, Italy; gimelli@ftgm.it 1071-3581/\$34.00

Copyright © 2017 American Society of Nuclear Cardiology.

INTRODUCTION

Left ventricular (LV) mechanical dyssynchrony has become a novel cardiac functional parameter, characterized by an adverse clinical and prognostic impact,^{1,2} independently from the presence of LV systolic dysfunction.^{2–5} Phase analysis on single-photon emission computed tomography (SPECT) imaging allows to quantify the presence of LVD, giving the chance to assess simultaneously LV perfusion and mechanics.^{6,7} The introduction of Cadmium-Zinc-Telluride (CZT) cameras has represented a significant breakthrough in nuclear cardiology, allowing a significant improvement in image quality despite a radical reduction of radiation burden and acquisition times.^{8,9} Using this novel technology, it has been demonstrated that the presence of LVD may associate with alterations of LV perfusion and function, independently from LV systolic function and coronary artery disease (CAD) extent.^{10,11} Interestingly, an association between the presence of LVD and alterations of LV sympathetic innervation has also been hypothesized.^{12,13} Nuclear imaging allows performing a non-invasive evaluation of LV regional adrenergic tone through the use of a highly specific radiotracer, namely ¹²³I-metaiodobenzylguanidine (¹²³I-MIBG).^{14–16} Moreover, the feasibility of a combined evaluation of myocardial innervation and perfusion within the same imaging session has been also demonstrated,^{15,16} allowing the assessment of the burden of abnormally innervated albeit viable LV myocardium (i.e., “innervation/perfusion” mismatch), a possibly innovative risk marker in different patient categories.^{16,17} In particular, a comprehensive evaluation of the relationships between regional LV perfusion, adrenergic innervation, and mechanics is still lacking. Accordingly, our specific hypothesis was that the presence of LVD might associate with regional alterations of myocardial sympathetic innervation and a higher burden of “innervation/perfusion” mismatch, possibly localizing at the level of the most dyssynchronous LV walls. Therefore, we aimed at assessing the interactions between regional myocardial “innervation/perfusion” imbalance and LVD in patients submitted to low-dose, ¹²³I-MIBG/^{99m}Tc-Tetrofosmin imaging on a dedicated cardiac CZT camera.

MATERIALS AND METHODS

Patient Population

We selected retrospectively all the 83 consecutive subjects that underwent myocardial perfusion imaging, with resting gated ^{99m}Tc-tetrofosmin tomographic acquisition on a dedicated CZT camera (Discovery NM 530c; GE Healthcare;

Haifa, Israel), and cardiac adrenergic innervation imaging by means of ¹²³I-MIBG CZT scintigraphy followed by standard planar acquisition between 2013 and 2016 in our institution. Both planar and tomographic acquisitions were performed on the same day. The exclusion criteria were haemodynamic instability or severely symptomatic heart failure (NYHA Class IV), active myocardial inflammatory/infective disease, a recent (<6 months) cardiovascular and/or cerebrovascular event, and previous open-heart surgery. The study was approved by the local Ethical Committee and conformed to the Declaration of Helsinki on human research. Written informed consent was obtained from every patient.

Study Protocol

Patients underwent ¹²³I-MIBG CZT tomographic evaluation followed by a planar acquisition on a standard camera and subsequently ^{99m}Tc-tetrofosmin rest CZT acquisition using a single-day protocol (55–111 MBq for innervation and 185–259 MBq for perfusion scan). Fifteen minutes after the administration of the ¹²³I-MIBG, a tomographic acquisition of 10 minutes was performed.^{12,15,16} A 10-minutes planar image of the anterior thorax was then acquired using a dual-headed gamma camera (E.Cam; Siemens Medical Solution; Hoffman Estates, IL, USA), equipped with a low-energy all-purpose parallel-hole collimator. All images were acquired with a 128 × 128 matrix and a 20% energy window centered at the 159 keV photopeak of ¹²³I. Repeat planar and CZT studies were acquired 4 h after injection.¹⁵ Fifteen minutes after the delayed ¹²³I-MIBG acquisition, all patients underwent the ^{99m}Tc-tetrofosmin CZT scan, lasting 8 minutes.^{12,15} Acquisitions were anticipated, when necessary, by the administration of sublingual nitrates. Images were reconstructed on a standard workstation (Xeleris II; GE Healthcare) using a previously validated dedicated iterative algorithm with 50 iterations. A Butterworth post-processing filter (frequency 0.37 cycles/cm, order 7) was applied to the reconstructed slices, without scatter or attenuation correction.

Analysis of Innervation and Perfusion Images

From anterior planar ¹²³I-MIBG scintigraphic images, the early and late heart-to-mediastinum (H/M) count ratios were calculated as the ratios of the average counts per pixel of the respective ROIs.^{13,14} The ¹²³I-MIBG washout rate was computed after correction for background activity and without time-decay correction.

^{99m}Tc-tetrofosmin and ¹²³I-MIBG CZT images were scored semi-quantitatively using the same 17-segment LV model and a five-point scale using a commercially available software (Corridor4DM; Invia, Ann Arbor, MI). The scores corresponded approximately to 0 = normal (100% to 70% uptake), 1 = mild (69% to 50% uptake), 2 = moderate (49% to 30% uptake), 3 = severe reduction of radioisotope uptake (29% to 10% uptake), and 4 = absence of detectable tracer uptake (<10% uptake);¹⁸ however, they could be modified according to clinical judgment based on all other factors (i.e.,

the presence of attenuation in regions with normal function).^{18,19} A region was considered non-viable if showing a <50% ^{99m}Tc-tetrofosmin uptake with abnormal LV motion/thickening on gated images. Thus the summed rest score (SRS) and the summed ¹²³I-MIBG score (SS-MIBG) were calculated by adding the segmental scores of the perfusion and innervation images, respectively.¹⁵ Scoring was performed independently by two experienced nuclear physicians (AG and PM) and consensus was reached in case of divergence. As previously reported, only the early ¹²³I-MIBG SPECT dataset was used for further analyses.^{12,15,16}

Assessment of the Presence of “Innervation/Perfusion” Mismatch

The presence of “innervation/perfusion” mismatch was defined according to the segmental distributions of ^{99m}Tc-tetrofosmin and ¹²³I-MIBG: relative uptake of ^{99m}Tc-tetrofosmin—¹²³I-MIBG $\geq 25\%$. This conservative cut-off corresponded approximately to a one-point difference of the semi-quantitative scale used for regional perfusion and innervation.²⁰ In every patient, the number of LV segments (from 0 to 17) showing relative “innervation/perfusion” mismatch was recorded. In order to account for the frequent relative reduction of radiotracer uptake at the level of the inferior LV wall, the innervation at the level of the inferior LV wall was considered normal if signs of tissue attenuation were detected (i.e., reduced ^{99m}Tc-tetrofosmin uptake in regions with normal function). In addition, a regional evaluation of myocardial perfusion and innervation was also performed using the same software (Corridor4DM; Invia, Ann Arbor, MI)¹¹ and a five-region LV model (anterior, lateral, inferior, and septal wall and the apex).¹² For each wall, the percentage of the peak ^{99m}Tc-tetrofosmin and ¹²³I-MIBG uptakes was computed and the number of segments showing an “innervation/perfusion” mismatch defined.²¹ In order to account for the relative dimension of the different LV walls, the burden of myocardium showing an “innervation/perfusion” mismatch was also expressed as % of the total LV wall extent.

Analysis of LV Function

End-diastolic volume (EDV), end-systolic volume, and ejection fraction (EF) were automatically calculated from 16-frames reformatted images using a commercially available software (Corridor4DM, Invia, Ann Arbor, MI).^{22,23} On phase analysis, the time to peak myocardial contraction (TTP), defined as the percentage of the cardiac cycle at which the contraction is maximal, was computed, and the standard deviation (SD) of the phase distribution and the histogram bandwidth, during which 95% of myocardium initiated contraction, were automatically generated as measures of LVD.^{11,12} In order to obtain comparable values of SD and histogram bandwidth as in the literature,^{3,11} those two measures of LVD were converted into degrees by multiplying the values of percentages by 3.6 (360/100). The presence of LVD was diagnosed when the phase bandwidth and/or the SD exceeded by two SDs the previously published reference values for healthy men (bandwidth $89 \pm 38^\circ$; SD $20 \pm 10^\circ$) and women (bandwidth $88 \pm 31^\circ$; SD $21 \pm 11^\circ$) obtained with the same CZT device and imaging

protocol.¹¹ For the per-wall analysis, in patients with LVD, the region of latest mechanical activation of the LV myocardium (i.e., the one with the most delayed activation from the TTP) was automatically identified by the software algorithm using the same five-region LV model of the perfusion and innervation studies, as previously reported.¹² If the region of latest mechanical activation involved two continuous LV walls, they were both considered dyssynchronous. Moreover, when the latest contracting region was represented by the apex, the most delayed nearby myocardial wall was considered in subsequent analyses.

Statistical Analysis

Continuous variables were expressed as mean \pm SD, and categorical variables as percentages. Groups were compared for categorical data using Fisher’s exact test and for continuous variables using the analysis of variance followed by the Fisher’s protected least significant difference for multiple comparisons. All tests were two-sided; a $P < 0.05$ was considered to be significant. Logistic regression models were used to identify the predictors of the presence of LVD. For each variable, the odds ratio (OR) with the respective 95% confidence interval (CI) was reported. Statistical analyses were performed using JMP statistical software (SAS Institute Inc, version 4.0.0) and Stata software (Stata Statistical Software: Release 10, StataCorp. 2007, College Station, TX).

RESULTS

The demographical and clinical characteristics of the overall population and of the patients divided according to the presence of LVD are reported in Table 1. LVD was revealed in 36 (43%) patients, while LBBB was present in 8 patients (10%). The two groups were comparable regarding major clinical parameters and cardiovascular risk factors.

Relationships Between LV Dyssynchrony, Innervation, and Perfusion: Patient-Based Analysis

Patients with LVD showed more abnormal myocardial functional and structural parameters than those with normal LV contraction (Table 2). The presence of LVD clustered with more altered measures of LV perfusion and sympathetic innervation heterogeneity (i.e., SRS and SS-MIBG; Table 2). In the overall population, significant correlations between measures of LVD at phase analysis and both innervation and perfusion parameters were revealed (Figure 1). When the regional distribution of LV perfusion and innervation was analyzed, most of the patients showed regions of “innervation/perfusion” mismatch on an average of 7 ± 3 LV segments. Interestingly, as shown in Figure 2, a significant association was evident between the presence of LVD and the burden of “innervation/perfusion” mismatch. On multivariate

Table 1. Characteristics of the patients

Parameter	Overall population (n = 83)	LV dyssynchrony		P value
		Absent (n = 47)	Present (n = 36)	
Age (years)	69 ± 11	69 ± 10	69 ± 10	0.929
Men	58 (70%)	27 (57%)	31 (86%)	0.010
Ischemic heart disease	63 (76%)	34 (72%)	29 (81%)	0.445
Left-bundle branch-block	8 (10%)	1 (2%)	7 (19%)	0.019
Family history of coronary artery disease	37 (45%)	17 (36%)	20 (56%)	0.118
Diabetes	30 (36%)	15 (32%)	15 (42%)	0.369
Hypercholesterolemia	51 (61%)	29 (62%)	22 (61%)	0.999
Hypertension	57 (69%)	32 (68%)	25 (69%)	0.999
Smoking	37 (45%)	16 (34%)	21 (58%)	0.044
Obesity	10 (12%)	6 (13%)	4 (11%)	0.999

Bold values indicate statistical significance ($P < 0.05$)

Table 2. LV functional data

Parameter	LV dyssynchrony		P value
	Absent (n = 47)	Present (n = 36)	
LV volumes and function at rest			
End-diastolic volume, mL	127 ± 58	222 ± 79	<0.001
End-systolic volume, mL	63 ± 46	160 ± 73	<0.001
Ejection fraction, %	54 ± 15	28 ± 10	<0.001
LV dyssynchrony parameters			
Phase standard deviation, degrees	23 ± 9	55 ± 10	<0.001
Phase histogram bandwidth, degrees	62 ± 32	133 ± 57	<0.001
Perfusion data			
Summed rest score	10 ± 8	21 ± 9	<0.001
LV Sympathetic innervation data			
Early H/M ratio	1.6 ± 0.2	1.5 ± 0.2	0.014
Late H/M ratio	1.5 ± 0.2	1.4 ± 0.2	0.013
¹²³ I-MIBG washout rate	23 ± 14	26 ± 11	0.503
SS-MIBG	17 ± 11	29 ± 9	<0.001

Bold values indicate statistical significance ($P < 0.05$)

H/M, heart-to-mediastinum; ¹²³I-MIBG, ¹²³I-metaiodobenzylguanidine; SS-MIBG, summed ¹²³I-MIBG score

analysis, the extent of “innervation/perfusion” mismatch resulted, together with a depressed EF, the major predictor of LVD (Table 3).

Relationships Between LV Dyssynchrony, Innervation, and Perfusion: Wall-Based Analysis

In patients with LVD, the region of latest myocardial mechanical activation was located in the anterior,

lateral, inferior, or septal wall in 3 (7%), 14 (30%), 15(33%), and 14 (30%), respectively, involving 1 LV wall in 26 patients (72%) and 2 walls in the remainders. While the uptake of ^{99m}Tc-tetrofosmin did not vary significantly in regions with delayed mechanical activation, the myocardial uptake of ¹²³I-MIBG was gradually decreased in LV walls of patients without mechanical dyssynchrony, normally contracting walls of patients with mechanical dyssynchrony, and walls with delayed mechanical activation (Figure 3). Similarly, LV walls

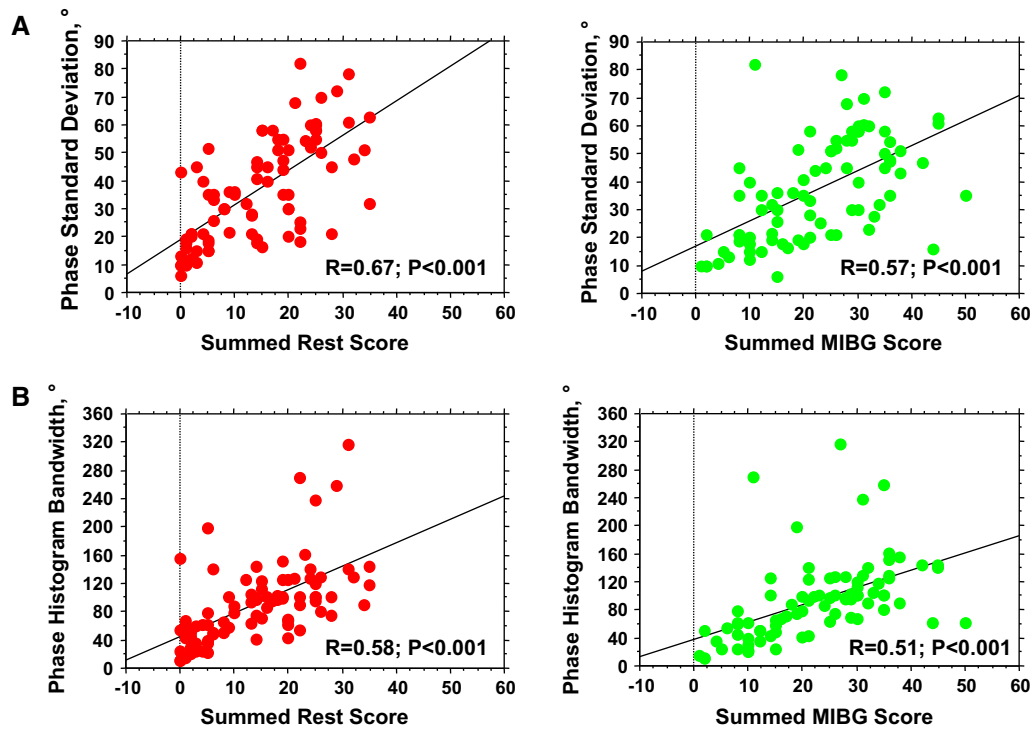


Figure 1. Relationships between measures of regional LV perfusion (*left panels*) and innervation (*right panels*) heterogeneities and measures of LVD: **A** phase standard deviation and **B** histogram bandwidth.

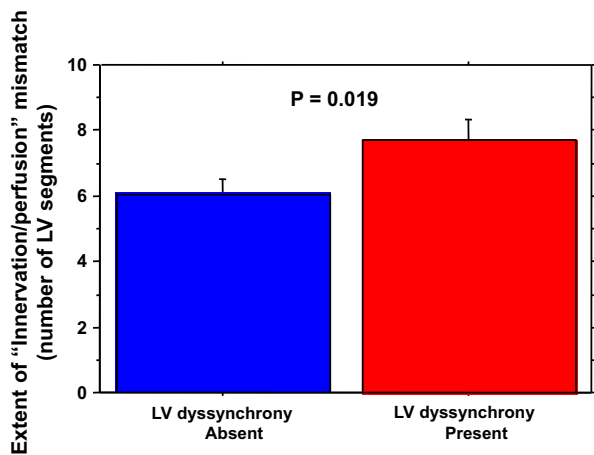


Figure 2. Interaction between LVD and the regional burden of “innervation/perfusion” mismatch in patients with (36 subjects; *red column*) and without (47 subjects; *blue column*) LVD.

showing a delayed mechanical activation also presented the highest burden of “innervation/perfusion” mismatch (Figure 3). On multivariate analysis, the presence and extent of “innervation/perfusion” mismatch was the only predictor of delayed regional myocardial activation [OR 1.46, 95% CI (1.04–2.06); $P = 0.029$],

overwhelming the effects of other functional parameters. A representative case of a patient with co-localized “innervation/perfusion” mismatch and delayed LV mechanical activation is shown in Figure 4.

DISCUSSION

LVD associates with the presence of significant LV functional impairment and clusters with relevant alterations of regional myocardial perfusion and sympathetic innervation. Patients with LVD show an extensive burden “innervation/perfusion” mismatch that is concentrated at the level of the dyssynchronous LV walls, suggesting a relationship between regional sympathetic denervation and abnormal LV mechanics.

Functional Predictors of LV Mechanical Dyssynchrony

While the presence of LVD is generally believed a prerogative of patients with compromised LV systolic function, a dyssynchronous myocardial mechanical activation may be revealed also in subjects with a normal EF, still predicting adverse cardiac prognosis.^{1–3,24} Nuclear cardiac imaging has represented a reference standard for the evaluation of LVD, phase

Table 3. Predictors of LV dyssynchrony

Variables	Univariate OR (95% CI)	P value	Multivariate OR (95% CI)	P value
Demographics and risk factors				
Age, years	1.00 (0.96-1.05)	0.927	NA	NA
Male sex, 1-0	4.59 (1.52-13.90)	0.007	NS	NS
Diabetes mellitus, 1-0	1.52 (0.62-3.76)	0.361	NA	NA
Hypercholesterolemia, 1-0	0.98 (0.40-2.38)	0.956	NA	NA
Hypertension, 1-0	1.07 (0.42-2.72)	0.895	NA	NA
Smoking, 1-0	2.71 (1.11-6.65)	0.029	NS	NS
Left-bundle branch-block, 1-0	11.10 (1.30-94.98)	0.028	NS	NS
Previous myocardial infarction, 1-0	0.49 (0.19-1.27)	0.144	NA	NA
LV functional parameters				
End-diastolic volume, mL	1.02 (1.01-1.03)	<0.001	NS	NS
End-systolic volume, mL	1.03 (1.02-1.05)	<0.001	NS	NS
Ejection fraction, %	0.86 (0.80-0.91)	<0.001	0.84 (0.77-0.91)	<0.001
Innervation and perfusion data				
Summed rest score	1.15 (1.08-1.22)	<0.001	NS	NS
Summed MIBG score	1.11 (1.06-1.17)	<0.001	NS	NS
Innervation/perfusion mismatch extent*	1.16 (1.01-1.32)	0.033	1.34 (1.06-1.67)	0.012

Bold values indicate statistical significance ($P < 0.05$)

LV, left ventricular; MIBG, ^{123}I -metaiodobenzylguanidine

* Number of LV segments

analysis being one of the first algorithms for its absolute quantification,⁷ and allowing the three-dimensional assessment of both LV perfusion and mechanical activation.^{11,12} Nevertheless, while various predictors of LVD have been reported,¹¹ few studies have insofar investigated the relative contribution of major cardiac functional parameters on the development of dyssynchronous LV mechanical contraction. Our data show that, in patients submitted to an integrated evaluation of myocardial contractile function, perfusion, and adrenergic innervation, LVD was ultimately predicted by the presence of significant regional innervation and perfusion abnormalities, overwhelming the effect of LV systolic function. In patients with LVD, while the walls showing the most delayed mechanical activation showed significantly abnormal measures of perfusion and adrenergic innervation, the extent of regional “innervation/perfusion” mismatch resulted as the strongest predictor of dyssynchronous mechanical activation.

LVD and Sympathetic Innervation

^{123}I -MIBG imaging represents the reference technique for the non-invasive depiction of cardiac adrenergic innervation, due to its elevated image quality, and low operative costs.²⁵ Moreover, when performed with dedicated CZT-based cardiac cameras, ^{123}I -MIBG

imaging can be performed easily with a few minutes acquisition time and a consistently reduced injected dose.¹⁵ In particular, the elevated photon sensitivity of CZT devices allows performing a combined evaluation of LV innervation and perfusion within the same imaging session and with a contained radiation burden (in the range of 3 mSv for the entire imaging protocol), possibly expanding the application of this technology to a wider arena of patients.^{12,16,20} Accordingly, initial reports have suggested that an abnormal LV sympathetic innervation at ^{123}I -MIBG imaging may associate with significantly depressed LV systolic function and predict the occurrence of LVD.^{12,13,26} Similarly, sympathetic denervation and LVD may interact in predicting patients events, possibly identifying subjects at higher risk of sudden cardiac death.²⁷ The present study shows that LVD associates with the presence of regional alterations of key parameters of myocardial perfusion and adrenergic innervation. In particular, those functional alterations were more prevalent at the level of dyssynchronous LV walls, suggesting a causal relationship between regional alterations of cardiac sympathetic innervation and LV mechanics. Moreover, our result suggests that the burden of abnormally innervated but viable LV myocardium, as a measure of regional “innervation/perfusion” mismatch might represent, more than the global extent of LV sympathetic

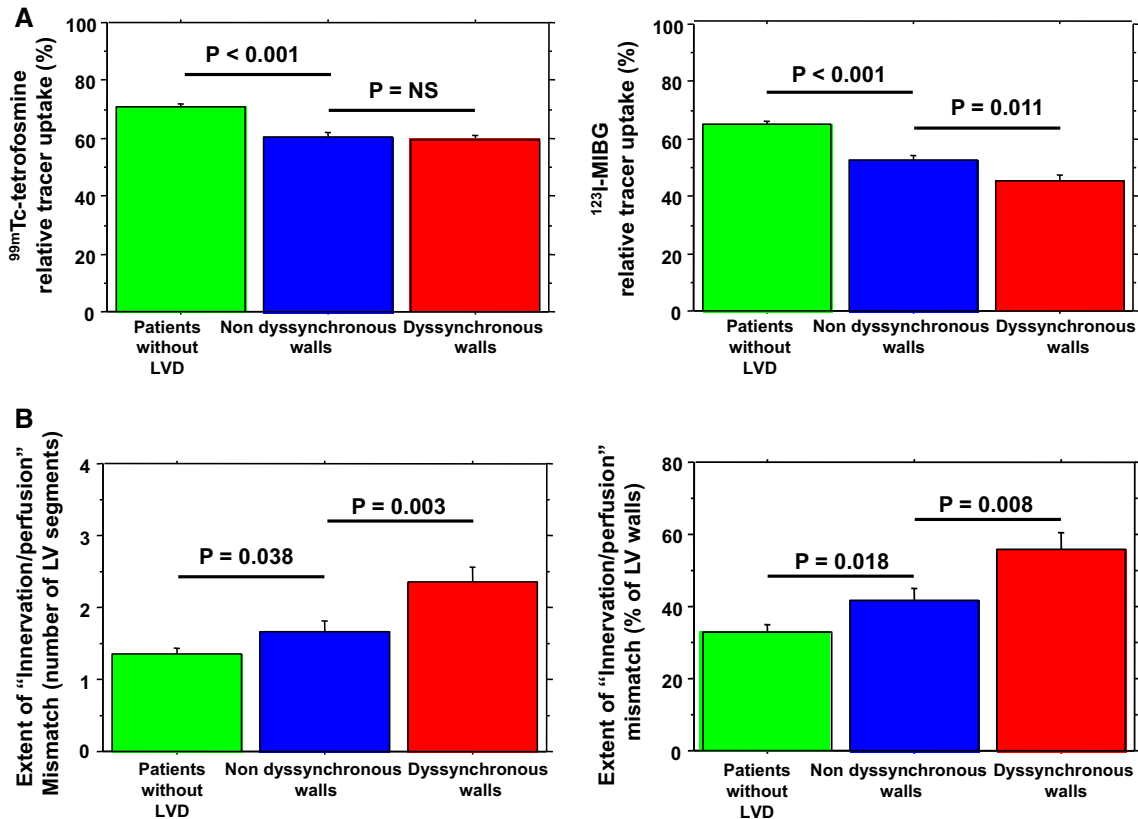


Figure 3. A Perfusion and innervation heterogeneity (relative tracer uptakes of ^{99m}Tc-tetrofosmin and ¹²³I-MIBG) and B extent of regional LV “innervation/perfusion” mismatch (number of mismatched segments and % of mismatched myocardium) in LV walls of patients without mechanical dyssynchrony (47 subjects; 188 walls), in normally contracting walls of patients with mechanical dyssynchrony (non-dyssynchronous walls; 98 walls), and in regions with delayed mechanical activation (dyssynchronous walls; 46 walls).

denervation itself, the strongest predictor of LVD, co-localizing with the regions of most delayed mechanical activation.

“Innervation/Perfusion” Mismatch and Cardiac Functional Impairment

It has been suggested that the burden of myocardial regions characterized by an “innervation/perfusion” mismatch might represent a risk marker for future cardiac events.^{16,17,28} Our results add further evidence in favor of the possible deleterious role of LV “innervation/perfusion” mismatch on cardiac function. In our population, an increasing burden of “innervation/perfusion” mismatch was the major predictor of the occurrence of LVD, independent of LV functional and structural parameters and of the extent of myocardial scar. Specifically, the distribution of regions with “innervation/perfusion” mismatch was deeply

inhomogeneous, identifying specifically the location of the most dyssynchronous LV walls. Present and previous evidences confirm the role of regional LV sympathetic denervation, as readily assessable through ¹²³I-MIBG SPECT, in cardiac pathology,^{12,13,16} underlining the impact of myocardial “innervation/perfusion” mismatch as an innovative marker of LV functional impairment and predictor of adverse cardiac risk.

LIMITATIONS

Since stress acquisition was not performed, the possible effect of underlying inducible ischemia on LVD cannot be excluded. However, all the patients with ischemic heart disease enrolled in the present study had no clinical evidence of residual ischemia and all of them had no signs of hemodynamically significant CAD at a recent (6-to-12 months before the CZT study) coronary

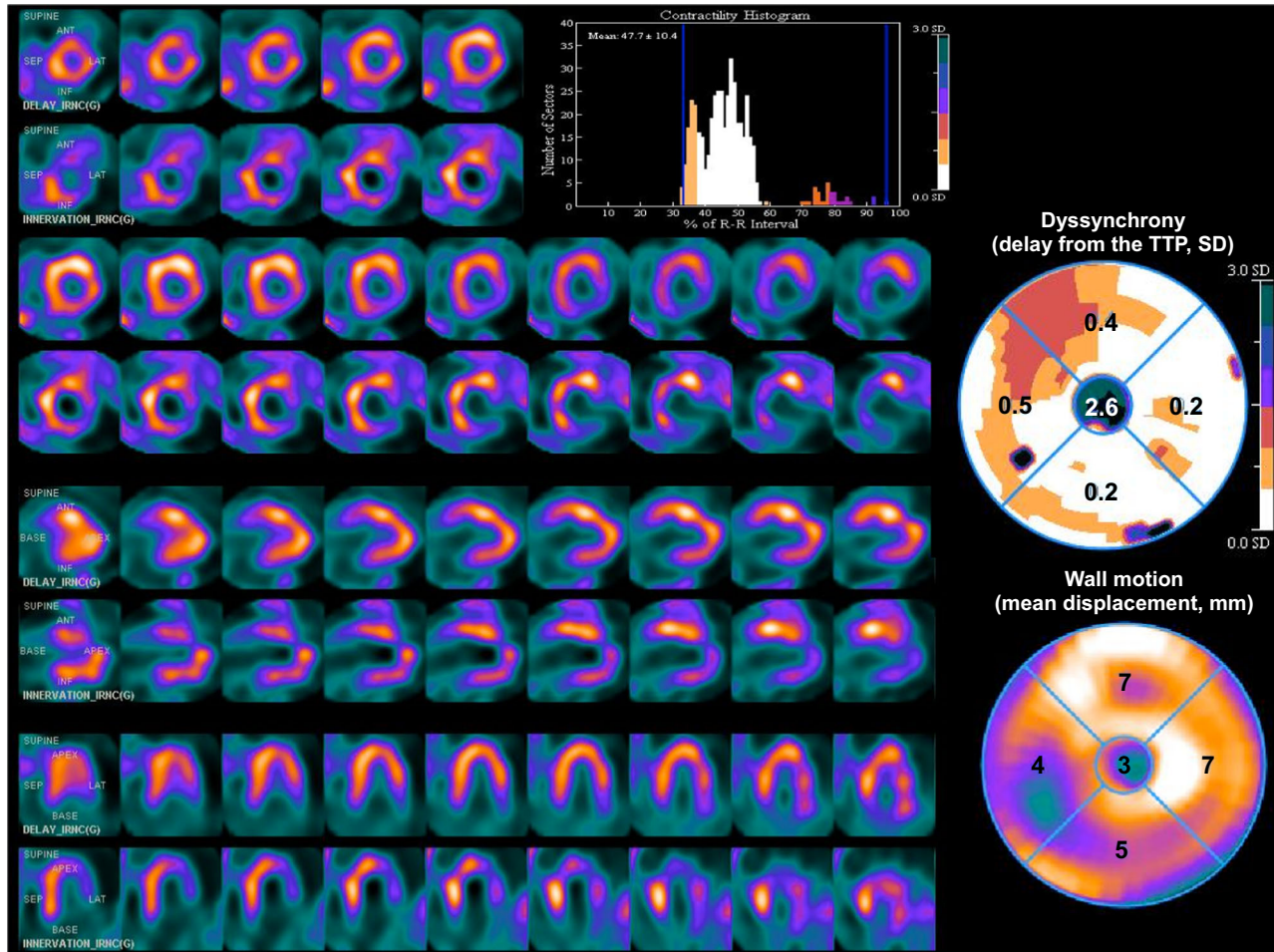


Figure 4. ^{99m}Tc -tetrofosmin images (upper rows) show a small basal inferior-to-inferolateral perfusion defect. ^{123}I -MIBG images (lower rows) show an area of sympathetic denervation at the level of the necrotic myocardium (“innervation/perfusion” match) and another wide region of impaired sympathetic tone at the level of the anterior, anteroseptal-to-apical LV segments despite a preserved perfusion (“innervation/perfusion” mismatch). LVD is depicted by means of a contractility histogram (upper left panel) and a phase bull’s eye (upper right panel) where the delay from the region of earliest mechanical activation is depicted in terms of increasing SD from TTP (0.2 SD for the lateral and inferior walls; 0.4, 0.5, and 2.6 SD for the anterior wall, septal wall, and the apex, respectively). In this case, it demonstrates the presence of LVD with the regions of more delayed activation localized at the level of the anteroseptal wall and of the apex, co-localizing with the mismatched regions. Notice that, although hypokinetic because of a basal scar (right panels), the inferior wall is not dyssynchronous as a possible result of tethering from the nearby viable myocardium. Specifically, the “Wall Motion” polar map reports the mean displacement in millimeters of the different LV walls (7 mm for the anterior and lateral walls; 5, 3, and 3 mm for the inferior wall, septal wall, and apex, respectively).

angiography. In the absence of accepted normalcy values of SD and histogram bandwidth in patients imaged on a CZT device, the presence of LVD was based on previously published cut-off values derived in a normal population studies with the same solid-state camera.¹¹ Nevertheless, despite this theoretical limitation, the values of SD and histogram bandwidth of patients with LVD enrolled in the present study were comparable with those reported in previous series.^{27,29}

The presence of an overall reduced cardiac uptake of MIBG (as expressed by a low H/M ratio) may impact negatively the quality of images obtained with traditional SPECT devices. However, the elevated image quality of ^{123}I -MIBG CZT acquisitions has been already demonstrated in a similar clinical setting, suggesting the feasibility of this imaging technique also in patients with a wide range of H/M ratios.^{12,15} Therefore, according to present and previous reports, the SS-MIBG seems of

particular value also in patients with enlarged LV and relatively reduced H/M ratios.^{20,28} The frequently reduced ¹²³I-MIBG uptake that is observed at the level of the inferior LV wall might have impacted negatively the evaluation of the “innervation/perfusion” mismatch. However, “innervation/perfusion” mismatch was excluded by protocol in the presence of signs of tissue attenuation on perfusion images. Accordingly, on per-wall analysis, the presence of “innervation/perfusion” mismatch co-localized with LVD, being relatively less represented on the anterior LV wall, which was involved infrequently by LVD (7% of the cases), than on the remaining walls (Suppl. Figure 1 in Electronic supplementary material 2). Similarly, no automated normalization of ^{99m}Tc-tetrofosmin and ¹²³I-MIBG counts was performed. In this respect, while the feasibility of an automated algorithm for the combined normalization of perfusion and innervation uptakes has been recently demonstrated,³⁰ no such algorithm has been implemented in the available software. Since no attenuation correction was used the accurate assessment of myocardial viability could have been hampered. However, it has been already demonstrated that the integration of LV perfusion and wall motion data coming from gated SPECT analysis can allow an efficient discrimination of attenuation artifacts and definition of regional myocardial viability.¹⁹

CONCLUSIONS

Patients with LVD show significant alterations of regional myocardial perfusion and sympathetic innervation. Specifically, the presence of a dyssynchronous LV contraction associates with a higher burden of “innervation/perfusion” mismatch that concentrates at the level of the LV walls with delayed mechanical activation, suggesting a close relationship between regional sympathetic denervation and abnormal LV mechanics.

NEW KNOWLEDGE GAINED

While the presence of LVD has been already shown to associate with some alterations of myocardial perfusion and adrenergic tone, the possible interaction between LV mechanics, perfusion, and innervation has never been evaluated. Present data suggest that patients with LVD show a significant extent of dysinnervated myocardium with relatively preserved perfusion that is mostly located at the level of the most dyssynchronous LV walls, linking the presence of localized LV sympathetic denervation with the development of regional LV contractile abnormalities.

Compliance with Ethical Standards

Disclosure

The authors have no conflicts of interest to disclose.

References

1. Bax JJ, Bleeker GB, Marwick TH, Molhoek SG, Boersma E, Steendijk P, et al. Left ventricular dyssynchrony predicts response and prognosis after cardiac resynchronization therapy. *J Am Coll Cardiol* 2004;44:1834-40.
2. Hess PL, Shaw LK, Fudim M, Iskandrian AE, Borges-Neto S. The prognostic value of mechanical left ventricular dyssynchrony defined by phase analysis from gated single-photon emission computed tomography myocardial perfusion imaging among patients with coronary heart disease. *J Nucl Cardiol* 2017;24:482-90.
3. AlJaroudi W, Aggarwal H, Venkataraman R, Heo J, Iskandrian AE, Hage FG. Impact of left ventricular dyssynchrony by phase analysis on cardiovascular outcomes in patients with end-stage renal disease. *J Nucl Cardiol* 2010;17:1058-64.
4. Leong DP, Chakrabarty A, Shipp N, Molaee P, Madsen PL, Joerg L, et al. Effects of myocardial fibrosis and ventricular dyssynchrony on response to therapy in new-presentation idiopathic dilated cardiomyopathy: Insights from cardiovascular magnetic resonance and echocardiography. *Eur Heart J* 2012;33:640-8.
5. Morris DA, Vaz Pérez A, Blaschke F, Eichstädt H, Ozcelik C, Haverkamp W. Myocardial systolic and diastolic consequences of left ventricular mechanical dyssynchrony in heart failure with normal left ventricular ejection fraction. *Eur Heart J Cardiovasc Imaging* 2012;13:556-67.
6. Dauphin R, Nonin E, Bontemps L, Vincent M, Pinel A, Bonijoly S, et al. Quantification of ventricular resynchronization reserve by radionuclide phase analysis in heart failure patients: A prospective long-term study. *Circ Cardiovasc Imaging* 2011;4:114-21.
7. Nakajima K, Okuda K, Matsuo S, Kiso K, Kinuya S, Garcia EV. Comparison of phase dyssynchrony analysis using gated myocardial perfusion imaging with four software programs: Based on the Japanese Society of Nuclear Medicine working group normal database. *J Nucl Cardiol* 2017;24:611-21.
8. Gimelli A, Liga R, Duce V, Kusch A, Clemente A, Marzullo P. Accuracy of myocardial perfusion imaging in detecting multi-vessel coronary artery disease: A cardiac CZT study. *J Nucl Cardiol* 2016. doi:10.1007/s12350-015-0360-8.
9. Gimelli A, Bottai M, Giorgetti A, Genovesi D, Kusch A, Ripoli A, et al. Comparison between ultrafast and standard single-photon emission CT in patients with coronary artery disease: A pilot study. *Circ Cardiovasc Imaging* 2011;4:51-8.
10. Pazhenkottil AP, Buechel RR, Herzog BA, Nkoulou RN, Valenta I, Fehlmann U, et al. Ultrafast assessment of left ventricular dyssynchrony from nuclear myocardial perfusion imaging on a new high-speed gamma camera. *Eur J Nucl Med Mol Imaging* 2010;37:2086-92.
11. Gimelli A, Liga R, Giorgetti A, Favilli B, Pasanisi EM, Marzullo P. Determinants of left ventricular mechanical dyssynchrony in patients submitted to myocardial perfusion imaging: A cardiac CZT study. *J Nucl Cardiol* 2016;23:728-36.
12. Gimelli A, Liga R, Genovesi D, Giorgetti A, Kusch A, Marzullo P. Association between left ventricular regional sympathetic denervation and mechanical dyssynchrony in phase analysis: A cardiac CZT study. *Eur J Nucl Med Mol Imaging* 2014;41:946-55.

13. Tanaka H, Tatsumi K, Fujiwara S, Tsuji T, Kaneko A, Ryo K, et al. Effect of left ventricular dyssynchrony on cardiac sympathetic activity in heart failure patients with wide QRS duration. *Circ J* 2012;76:382-9.
14. Jacobson AF, Senior R, Cerqueira MD, Wong ND, Thomas GS, Lopez VA, et al. Myocardial iodine-123 meta-iodobenzylguanidine imaging and cardiac events in heart failure. Results of the prospective ADMIRE-HF (AdreView Myocardial Imaging for Risk Evaluation in Heart Failure) study. *J Am Coll Cardiol* 2010;55:2212-21.
15. Gimelli A, Liga R, Giorgetti A, Genovesi D, Marzullo P. Assessment of myocardial adrenergic innervation with a solid-state dedicated cardiac cadmium-zinc-telluride camera: First clinical experience. *Eur Heart J Cardiovasc Imaging* 2014;15:575-85.
16. Gimelli A, Masci PG, Liga R, Grigoratos C, Pasanisi EM, Lombardi M, et al. Regional heterogeneity in cardiac sympathetic innervation in acute myocardial infarction: Relationship with myocardial oedema on magnetic resonance. *Eur J Nucl Med Mol Imaging* 2014;41:1692-4.
17. Fallavollita JA, Heavey BM, Luisi AJ Jr, Michalek SM, Baldua S, Mashtare TL Jr, et al. Regional myocardial sympathetic denervation predicts the risk of sudden cardiac arrest in ischemic cardiomyopathy. *J Am Coll Cardiol* 2014;63:141-9.
18. Kapur A, Latus KA, Davies G, Dhawan RT, Eastick S, Jarritt PH, et al. A comparison of three radionuclide myocardial perfusion tracers in clinical practice: The ROBUST study. *Eur J Nucl Med Mol Imaging* 2002;29:1608-16.
19. Genovesi D, Giorgetti A, Gimelli A, Kusch A, D'Aragona Tagliavia I, Casagrande M, et al. Impact of attenuation correction and gated acquisition in SPECT myocardial perfusion imaging: Results of the multicentre SPAG (SPECT Attenuation Correction vs Gated) study. *Eur J Nucl Med Mol Imaging* 2011;38:1890-8.
20. Gimelli A, Liga R, Avogliero F, Coceani M, Marzullo P. Relationships between left ventricular sympathetic innervation and diastolic dysfunction: The role of myocardial innervation/perfusion mismatch. *J Nucl Cardiol* 2016. doi:10.1007/s12350-016-0753-3.
21. Cerqueira MD, Weissman NJ, Dilsizian V, Jacobs AK, Kaul S, Laskey WK, et al. Standardized myocardial segmentation and nomenclature for tomographic imaging of the heart. A statement for healthcare professionals from the Cardiac Imaging Committee of the Council on Clinical Cardiology of the American Heart Association. *Circulation* 2002;105:539-42.
22. Gimelli A, Liga R, Pasanisi EM, Giorgetti A, Marras G, Favilli B, et al. Evaluation of left ventricular diastolic function with a dedicated cadmium-zinc-telluride cardiac camera: Comparison with Doppler echocardiography. *Eur Heart J Cardiovasc Imaging* 2014;15:972-9.
23. Gimelli A, Liga R, Giorgetti A, Kusch A, Pasanisi EM, Marzullo P. Relationships between myocardial perfusion abnormalities and poststress left ventricular functional impairment on cadmium-zinc-telluride imaging. *Eur J Nucl Med Mol Imaging* 2015;42:994-1003.
24. Gorcsan J 3rd, Sogaard P, Bax JJ, Singh JP, Abraham WT, Borer JS, et al. Association of persistent or worsened echocardiographic dyssynchrony with unfavourable clinical outcomes in heart failure patients with narrow QRS width: A subgroup analysis of the EchoCRT trial. *Eur Heart J* 2016;37:49-59.
25. Boogers MJ, Borleffs CJ, Henneman MM, van Bommel RJ, van Ramshorst J, Boersma E, et al. Cardiac sympathetic denervation assessed with 123-iodine metaiodobenzylguanidine imaging predicts ventricular arrhythmias in implantable cardioverter-defibrillator patients. *J Am Coll Cardiol* 2010;55:2769-77.
26. Cha YM, Chareonthaitawee P, Dong YX, Kemp BJ, Oh JK, Miyazaki C, et al. Cardiac sympathetic reserve and response to cardiac resynchronization therapy. *Circ Heart Fail* 2011;4:339-44.
27. Hage FG, Aggarwal H, Patel K, Chen J, Jacobson AF, Heo J, et al. The relationship of left ventricular mechanical dyssynchrony and cardiac sympathetic denervation to potential sudden cardiac death events in systolic heart failure. *J Nucl Cardiol* 2014;21:78-85.
28. Gimelli A, Menichetti F, Soldati E, Liga R, Vannozzi A, Marzullo P, et al. Relationships between cardiac innervation/perfusion imbalance and ventricular arrhythmias: Impact on invasive electrophysiological parameters and ablation procedures. *Eur J Nucl Med Mol Imaging* 2016;43:2383-91.
29. Aljaroudi WA, Hage FG, Hermann D, Doppalapudi H, Venkataraman R, Heo J, et al. Relation of left-ventricular dyssynchrony by phase analysis of gated SPECT images and cardiovascular events in patients with implantable cardiac defibrillators. *J Nucl Cardiol* 2010;17:398-404.
30. Clements IP, Garcia EV, Chen J, Folks RD, Butler J, Jacobson AF. Quantitative iodine-123-metaiodobenzylguanidine (MIBG) SPECT imaging in heart failure with left ventricular systolic dysfunction: Development and validation of automated procedures in conjunction with technetium-99 m tetrofosmin myocardial perfusion SPECT. *J Nucl Cardiol* 2016;23:425-35.